

P1.20

Warm season extreme quantitative precipitation forecasting for the Burlington, VT region

John Gyakum¹, E. Atallah¹, P. Sisson², M. Kimball³, and A. Roberge¹
¹McGill University, ²NWSFO Burlington, VT, ³University of Utah

1. Introduction

The accurate forecasting of extreme precipitation events is a paramount concern as flooding is the leading weather related cause of the loss of life and property in the United States. As such, several studies have focused on identifying the triggers and synoptic-scale dynamics associated with heavy precipitation events, particularly those events requiring flood warnings.

LaPenta et al (1995) identified common characteristics of heavy precipitation and flooding events focusing on the eastern region of the National Weather Service. Triggering mechanisms as well as an ingredients based methodology for the production of flash flood forecasts were proposed by Doswell et al. (1996). Whitter et al. (2004) identified a possible mechanism for the formation of heavy rainfall events in the Burlington, VT region. Recently, Sisson and Gyakum (2004) found common characteristics among cold-season extreme precipitation events in the region. The purpose of this study is to extend the results of Sisson and Gyakum (2004) to the warm season and provide forecasters with precursor signatures for the identification of potentially hazardous rainfall.

2. Data and Methodology

The area under consideration for this study is defined by a box with a southwest corner of 43.5°N and 72°W and a northeast corner of 45°N and 74.25°W. This region was chosen to include the more densely populated regions of the Champlain Valley, as well as portions of the Adirondack and Green mountains. Heavy and extreme precipitation events were identified using statistics compiled from the Unified Precipitation Data Set (UPD). (For more details, please refer to <http://www.cdc.noaa.gov/cdc/data.unified.html>).

Extreme events are then defined as those exceeding two standard deviations above the mean, or 36.9 mm, whereas heavy events are defined by totals exceeding 24.2 mm but less than 36.9 mm. These thresholds yielded 25 dates where the extreme criteria was met and 462 dates where the heavy criteria was met. It should be noted that an event is identified when those thresholds are exceeded at any single grid point in the region.

¹ Corresponding author address: John Gyakum, Department of Atmospheric and Oceanic Sciences, McGill University, Montreal, QC: email: john.gyakum@mcgill.ca

In order to ensure that different events represented different synoptic-scale disturbances, a 7-day separation was imposed between different events. After applying the above conditions, 53 extreme events were kept. To ensure an equal amount of smearing or smoothing due to the compositing procedure, heavy cases were randomly eliminated, leaving a sample size of 53 to match the sample size of the extreme composite.

The National Centers for Environmental Prediction/National Centers for Atmospheric Research's (NCEP/NCAR) Global Reanalysis (Kalnay et al. 1996) was used for the purpose of compositing the dynamic and thermodynamic fields associated with the above events. A weighted, diurnal climatology was also created from the Reanalysis data set, with weighting dependent on the number of events in each of the warm season months.

However, due to the relatively coarse nature of the Global Reanalysis, some of the moisture/instability fields used in this study are composited from the North American Regional Reanalysis (NARR, for more details, please see <http://www.emc.ncep.noaa.gov/mmb/rrean/>). Since the NARR is only available back to 1979, composites involving the NARR are restricted to 32 members.

3. Results and Discussion

Figure 1 shows the potential temperature (θ) and winds on the dynamic tropopause (DT) as defined by the 2 potential vorticity units (PVU) surface for the composite of extreme events. At time $t = -60$ h (60 h before the 00 UTC time of the date of the event) there is an anomalously warm ridge on the DT roughly centered over the Mississippi River, with weak thermal troughs located over the Northeast and the Intermountain west (Fig. 1a). Twelve hours later the ridge has amplified and shifted slightly to the east, with a θ anomaly of over 4 K stretching from the upper Midwest to the Tennessee Valley (Fig 1b). A strong warm air advection signature is already evident over the northeast at this time. Note that as early as $t = -36$ h, the warm anomaly has started to overspread the region of interest (Fig. 1c). The ridge continues to amplify as it shifts towards the Northeast reaching an anomaly magnitude of over 6 K by time $t = -12$ h (Fig. 1e). At this time, the 345 K isentrope stretches from near Chicago, IL to Albany, NY, with a neutral to cold advection pattern over the Northeast. However, by time $t = 0$ h, the 345 K isentrope has

shifted to the north over the region, now lying across the New York/Quebec border (Fig. 1f). The non-conservation of θ on the DT is strongly suggestive of diabatic enhancement of the ridge due to latent heat release from precipitation in the area.

Figure 2 shows θ on the DT for the heavy composite. Two differences relative to the extreme composite are immediately evident. The first difference is that warm anomaly over the north central US is less pronounced than in the extreme composite (Fig. 2a). The second is the presence of a cool anomaly over Alberta and Saskatchewan indicative of a synoptic-scale trough. (However, it should be noted that the absence of this cold anomaly in the extreme composite is an artifact of smearing from the compositing process. Smearing is less of an issue in the heavy composite, as the events are less diverse in nature.) Twenty-four hours later, there is a cold/warm anomaly couplet organizing over the Northern Plains (Fig. 2c). Note that the warm anomaly does not start overspreading the Northeast until $t = -24$ h (Fig. 2d), twelve hours later than in the extreme composite. As in the extreme composite, the magnitude of the warm anomaly on the DT increases as the ridge propagates eastward, with a 4 K anomaly indicated over New York at $t = -12$ h (Fig. 2e). Non-conservation of θ on the DT is again evident in the final twelve hours of the evolution (Fig. 2f).

More traditional diagnostics are given in figure 3, which displays the mean sea-level pressure (mslp) and 1000-500 hPa thickness for the extreme composite. At time $t = -60$ the picture is dominated by the presence of the subtropical, oceanic high-pressure systems, typical of the warm season (Fig. 3a). The return flow on the western flank of the Bermuda high is transporting warm, moist air northward towards the Northern Plains. A weak trough is centered over the Northern Plains. A region of anomalously warm thickness values stretches from Kansas to southeastern Canada. The trough weakens somewhat as the system propagates to the east, although the magnitude of the warm thickness anomaly increases from 20 to 30 m (Fig. 3b). While the magnitude of the warm anomaly increases, the magnitude of the cool anomaly on the western flank of the trough diminishes as the system moves away from the front range of the Rockies (Fig. 3c). Twelve hours later, the magnitude of the warm anomaly has increased to 40 m and is now centered over southern Ontario (Fig. 3d). By time $t = -12$, the trough is centered over the western Great Lakes with warm air advection ahead of the trough

indicative of synoptic-scale forcing for ascent (fig. 3e).

Figure 4 displays the mslp and 1000-500 hPa thickness for the heavy composite. In stark contrast to the extreme composite, the heavy composite shows a cool thickness anomaly over the Northeast at time $t = -60$ h (Fig. 4a). While the magnitude of the warm anomaly increases over time, warm air advection only starts to overspread the region at $t = -12$ h (Fig. 4e).

In general, both the extreme and heavy composites are characterized by a warm ridge propagating into the Northeast from the Northern Plains and Upper Midwest. However, the ridging in the extreme composite is more persistent and larger in scale than in the heavy composite. This suggests that "priming" and thermodynamic instability is essential in discriminating between extreme and heavy events. This assertion is supported by an analysis of the moisture and instability fields taken from the NARR, but not shown here in the interest of brevity.

4. Acknowledgements

This research is supported through funding from the Cooperative Program for Operational Meteorology, Education and Training (COMET) and is a joint effort of The National Weather Service Forecast Office in Burlington, VT and McGill University.

5. References

- Doswell III, C. A., H. A. Brooks, and R. Maddox, 1996: Flash flood forecasting: An ingredients-based methodology. *Wea. Forecasting.*, **11**, 560–581.
- Kalnay, E. and coauthors 1996: The NCEP/NCAR 40-year reanalysis project. *Bull. Amer. Meteor. Soc.*, **77**, 437–471.
- LaPenta, K. and coauthors, 1995: The challenge of forecasting heavy rain and flooding throughout the eastern region of the National Weather Service. Part I: Characteristics and events. *Wea. Forecasting.*, **10**, 78-90.
- Sisson, P. A. and J. R. Gyakum, 2004: Synoptic-scale precursors to significant cold-season precipitation events in Burlington, Vermont. *Wea. Forecasting.*, **19**, 841–854.
- Whitter, S., G. Hanson, and R. Bell, 2004: A conceptual model of warm season excessive rainfall used to warn for flooding of 12 June 2002 across northern Vermont. Preprint P9.1, 11th Conference on Mountain Meteorology.

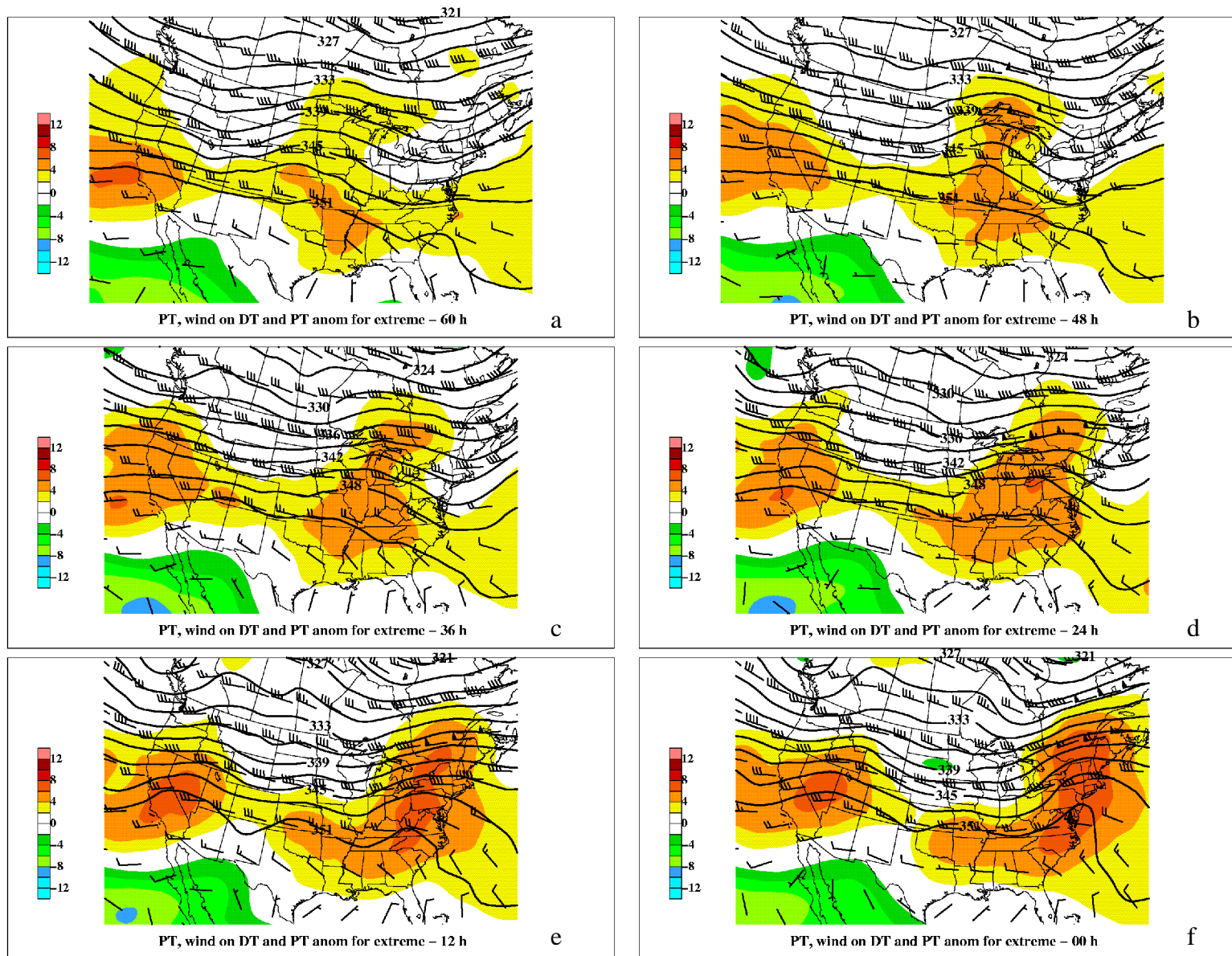


Figure 1. Potential Temperature (solid black lines, contoured every 3 K), PT anomaly (shaded every 2 K), and wind (barbs, knots convention) on the Dynamic Tropopause as defined by the 2 PVU surface for the extreme composite at time a) $t = -60$ h, b) $t = -48$ h, c) $t = -36$ h, d) $t = -24$ h, e) $t = -12$ h, and f) $t = 0$ h.

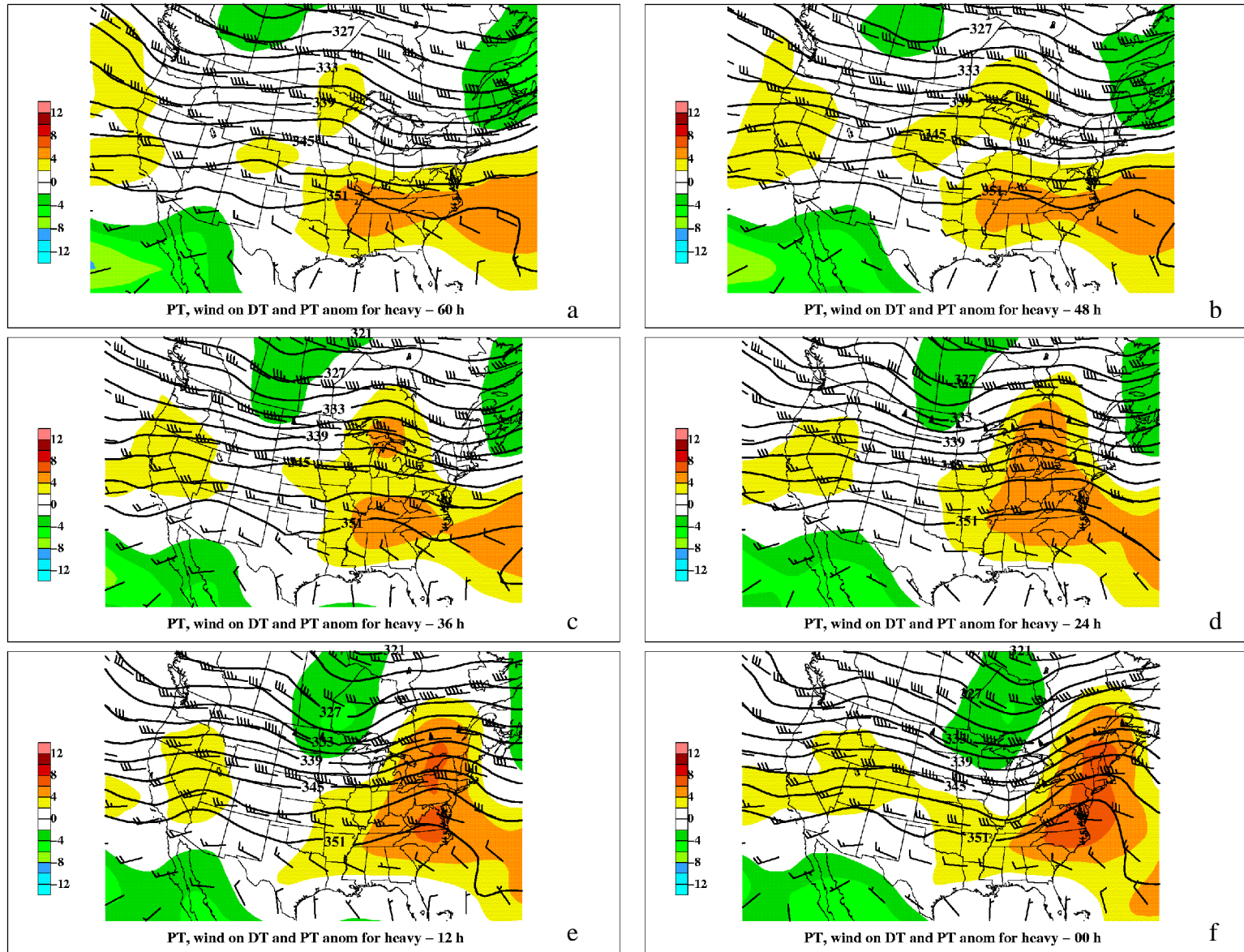


Figure 2. Potential Temperature (solid black lines, contoured every 3 K), PT anomaly (shaded every 2 K), and wind (barbs, knots convention) on the Dynamic Tropopause as defined by the 2 PVU surface for the heavy composite at time a) $t = -60$ h, b) $t = -48$ h, c) $t = -36$ h, d) $t = -24$ h, e) $t = -12$ h, and f) $t = 0$ h.

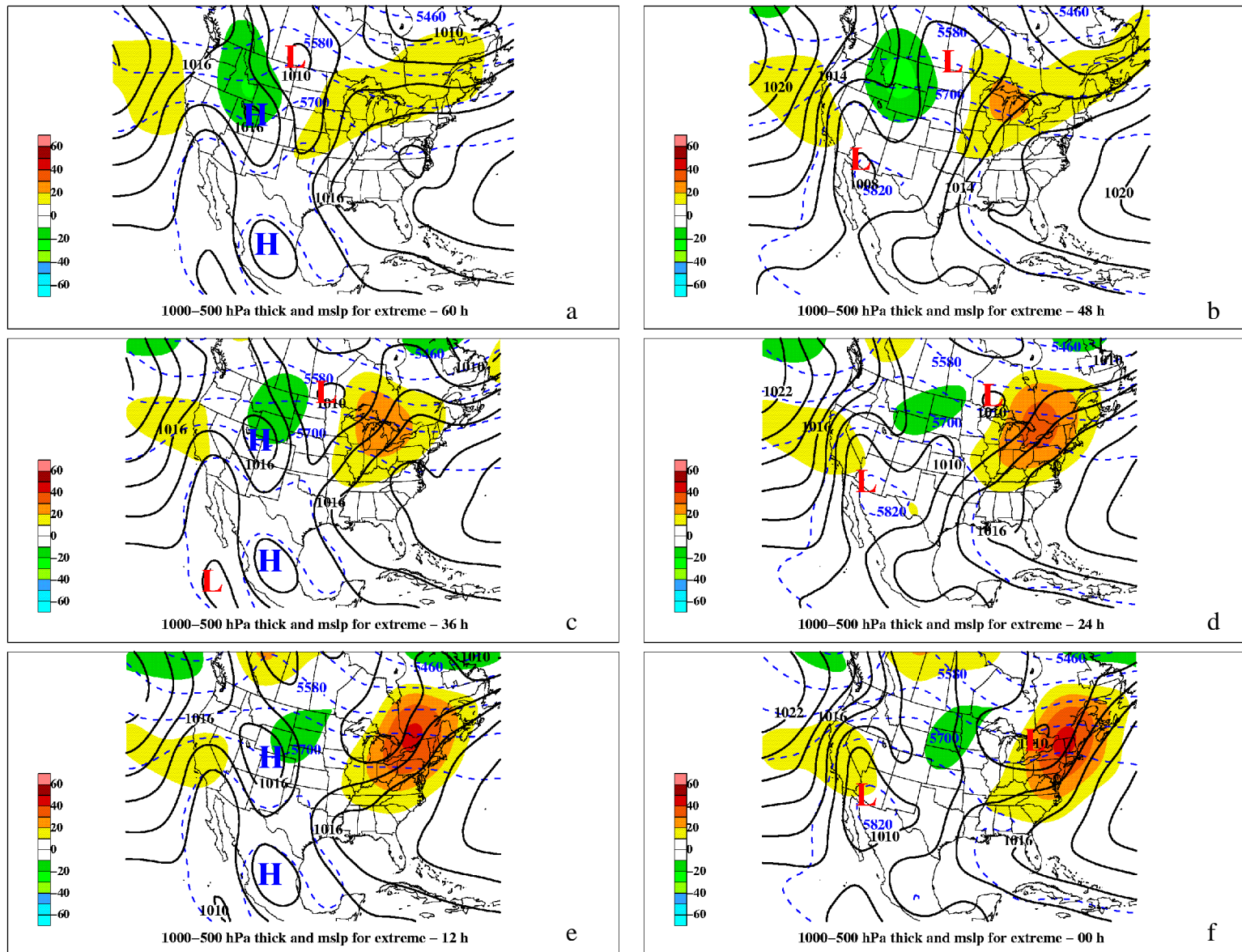


Figure 3. Mean Sea Level Pressure (solid black lines, contoured every 4 hPa), 1000-500 hPa thickness (dashed blue line, contoured every 6 dam, and thickness anomaly (shaded every 1 dam), for the extreme composite at time a) $t = -60$ h, b) $t = -48$ h, c) $t = -36$ h, d) $t = -24$ h, e) $t = -12$ h, and f) $t = 0$ h.

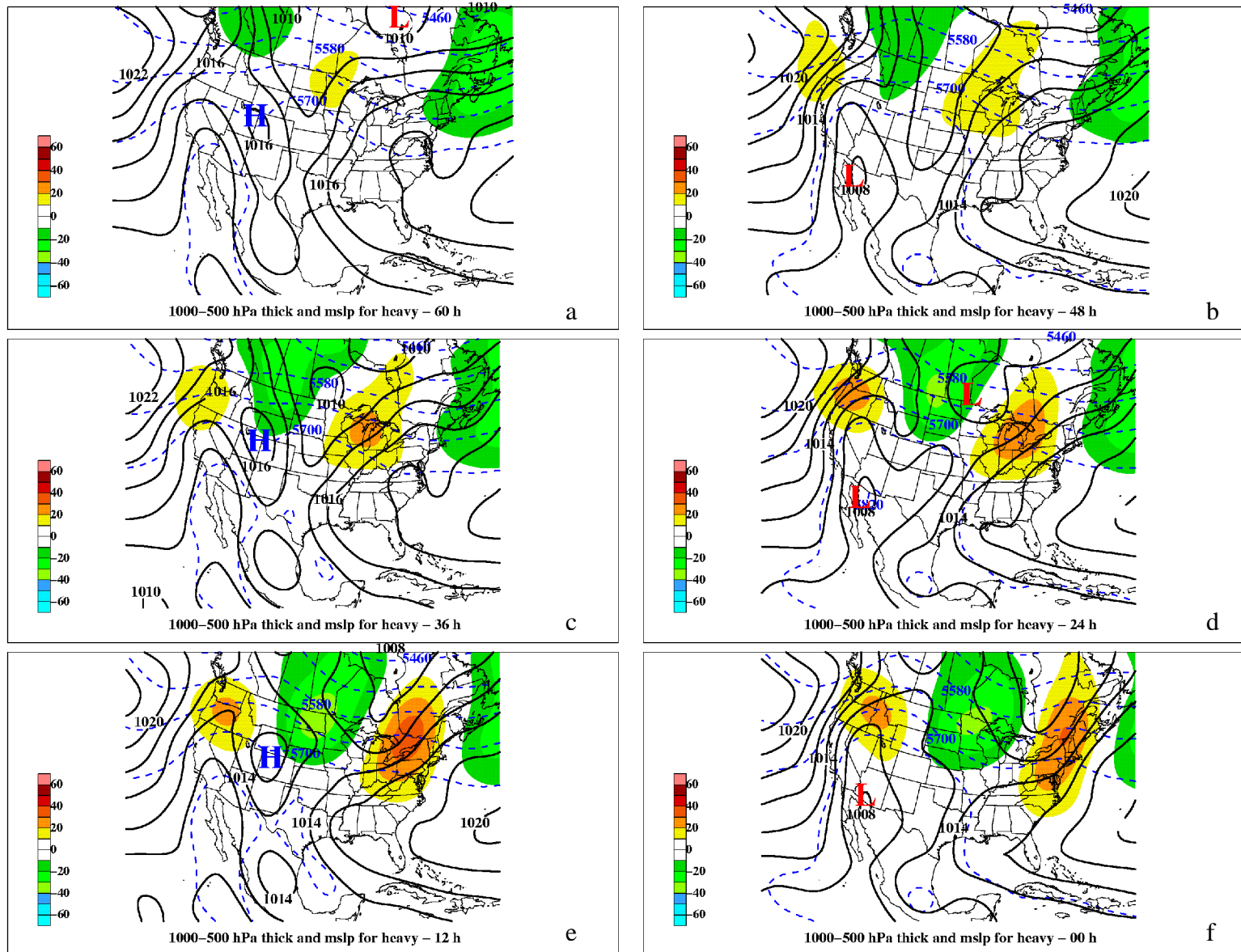


Figure 4. Mean Sea Level Pressure (solid black lines, contoured every 4 hPa), 1000-500 hPa thickness (dashed blue line, contoured every 6 dam, and thickness anomaly (shaded every 1 dam), for the heavy composite at time a) $t = -60$ h, b) $t = -48$ h, c) $t = -36$ h, d) $t = -24$ h, e) $t = -12$ h, and f) $t = 0$ h.